Nucleic Acids Research, 1994, Vol. 22, No. 3 301–307

Selective cleavage of *bcr-abl* chimeric RNAs by a ribozyme targeted to non-contiguous sequences

Catherine J.Pachuk[1], Kyonggeun Yoon[1], Karin Moelling[1,2,3] and Leslie R.Coney[1]
[1]Department of Molecular and Cellular Biology, Apollon, One Great Valley Parkway, Malvern, PA 19355, USA, [2]Max Planck Institut für Molekulare Genetik, Ihnestrasse 73, D1000 Berlin 33, Germany and [3]Institute of Medical Virology, Gloriastrasse 30, University, Zürich, Switzerland

Received November 3, 1993; Accepted December 22, 1993

ABSTRACT

Conventionally designed ribozymes may be unable to cleave RNA at sites which are inaccessible due to secondary structure. In addition, it may also be difficult to specifically target a conventionally designed ribozyme to some chimeric RNA molecules. Novel approaches for ribozyme targeting were developed by using the L6 *bcr-abl* fusion RNA as a model. Using one approach, we successfully directed ribozyme nucleation to a site on the *bcr-abl* RNA that is distant from the GUA cleavage site. These ribozymes bound to the L6 substrate RNA via an anchor sequence that was complementary to *bcr* sequences. The anchor was necessary for efficient cleavage as the anchor minus ribozyme, a conventionally designed ribozyme, was inefficient at catalyzing cleavage at this same site. The effect of anchor sequences on catalytic rates was determined for two of these ribozymes. Ribozymes generated by a second approach were designed to cleave at a CUU site in proximity to the *bcr-abl* junction. Both approaches have led to the development of a series of ribozymes specific for both the L6 and K28 *bcr-abl* chimeric RNAs, but not normal *abl* or *bcr* RNAs. The specificity of the ribozyme correlated in part with the ability of the ribozyme to bind substrate as demonstrated by gel shift analyses. Secondary structure predictions for the RNA substrate support the experimental results and may prove useful as a theoretical basis for the design of ribozymes.

INTRODUCTION

An important requirement for the development of ribozymes is the ability to specifically target a ribozyme to a cellular RNA of interest. This can be especially difficult when designing a ribozyme for a chimeric RNA molecule that is homologous to a another RNA molecule, particularly if cleavage of the second RNA is detrimental to the host. It may be equally difficult to target an RNA molecule that is folded in a way that prevents ribozyme interactions at or near the ribozyme cleavage site. We have encountered both of these problems in our attempts to design ribozymes that are specific for an aberrant mRNA associated with chronic myelogenous leukemia (CML).

CML is a clonal myeloproliferative disorder of hematopoietic stem cells associated with the Philadelphia chromosome (1); a chromosomal abnormality resulting from a translocation between chromosomes 9 and 22 (2). The breakpoints on chromosome 22 are clustered in a 6 kb region termed the breakpoint cluster region (*bcr*) (3), while on chromosome 9, the breakpoints are scattered throughout a 90 kb region upstream from c-*abl* exon 2 (4). The various 9:22 translocations that result can be subdivided into two types: K28 translocations and L6 translocations (Figure 1) (5).

In K28 translocations, the chromosome 22 breakpoints lie between *bcr* exons 3 and 4. Transcription through this region yields an hnRNA which can be alternately spliced to yield two distinct chimeric mRNAs: mRNA K28 and mRNA L6 (5). In mRNA K28, *bcr* exon 3 is fused to *abl* exon 2, while in mRNA L6, *bcr* exon 2 is fused to *abl* exon 2. In L6 translocations, the chromosomal breakpoints lie between *bcr* exons 2 and 3. Transcription through this region yields only one species of chimeric mRNA, mRNA L6 (5).

Chimeric RNAs can be ideal candidates for ribozyme targeting particularly when a ribozyme cleavage site is located within 2 or 3 nucleotides of the chimeric junction. In this case a ribozyme can be targeted specifically to the chimeric molecule by specifying that 1) ribozyme sequences 5′ of the catalytic region be complementary to chimeric RNA sequences located immediately 3′ of the cleavage site, and 2) ribozyme sequences 3′ of the catalytic region be complementary to chimeric sequences situated just 5′ of the cleavage site. The specificity of the ribozyme is thus maintained and the potentially harmful results of non-specific ribozyme cleavage avoided. However, not all chimeric mRNAs exhibit a convenient site for ribozyme cleavage. An examination of the L6 *bcr-abl* mRNA sequence reveals that the closest ribozyme cleavage sites in the vicinity of the *bcr-abl* junction are located 7, 8, and 19 nucleotides away from the junction (Figure 1B). Therefore, it may not be feasible to target any of these sites for ribozyme cleavage in the manner described because such ribozymes would likely also cleave normal *abl* mRNA or normal *bcr* mRNA. In addition, computer predictions for the secondary structures of L6 *bcr-abl* mRNA suggest that these sites may be inaccessible to these types of ribozymes. Accordingly,

we initiated new approaches to the design of ribozymes specific for L6 *bcr-abl* mRNA.

The experiments presented here were designed to determine the effect of these approaches on both ribozyme activity and specificity.

MATERIALS AND METHODS

Preparation of vector DNA

Bluescript II KS+ plasmid DNA (Stratagene) was digested to completion with either *Hinc* II or *Eco*R 1 (New England Biolabs) and dephosphorylated with Calf Intestinal Phosphatase (Boehringer Mannheim Biochemicals) according to conditions recommended by the supplier.

Construction and cloning of ribozyme DNAs

The DNA templates for each ribozyme were synthesized as two complementary oligodeoxynucleotides with *Eco*R 1 ends. Oligonucleotides were synthesized on a Milligen BioSearch 8750 DNA synthesizer by the phosphoramidite method (6) and subsequently purified by reverse phase High Pressure Liquid Chromatography (HPLC). Approximately 3 μg of each oligonucleotide were phosphorylated with T4 polynucleotide kinase (United States Biochemicals) according to conditions recommended by the manufacturer. Complementary oligonucleotides were annealed following phosphorylation and ligated into the *Eco*R 1 site of Bluescript II KS+. Ligated DNA was electroporated into HB101 bacteria using the 'Gene Pulser' (Bio-Rad) according to the manufacturer's instructions.

Construction and cloning of substrate DNAs

The DNA template for the L6 *bcr-abl* substrate RNA was synthesized as an oligodeoxynucleotide having the same polarity as L6 *bcr-abl* mRNA. This DNA oligonucleotide is comprised of a sequence that maps from a position located 57 nt 5′ of the *bcr-abl* junction to a position located 97 nts 3′ of the *bcr-abl* junction (5,7). Double stranded DNA was synthesized by the polymerase chain reaction (PCR) using 5′ and 3′ primers which have the following sequences: 5′ ATTGCGATAGGATTGAATTCAACTCGTGTGTGAAACTCCA 3′ and 5′ AATGCGATAGGATTGAATTCGTCCAGCGAGAAGGTTTTCC 3′, respectively (*Eco*R 1 sites are underlined). PCR products were gel purified, *Eco*R 1 digested, and then cloned into Bluescript II KS+ as already described.

The DNA template for normal *bcr* substrate RNA was synthesized as an oligodeoxynucleotide having the same polarity as *bcr* mRNA. Double stranded DNA was synthesized by PCR using 5′ and 3′ primers which have the following sequences: 5′ ATTGCGATAGGATTGAATTCAAGCTTAAGTGTTTCAGAAGCTTCTCCCTGACATCCGTGGAGCTGCA 3′ and 5′ AATGCGATAGGATTGAATTCCGGAGACTCATCATCTTCCTTATTGATGGTCAGCGGAATGC 3′, respectively. The resulting PCR product maps from position 554 to position 675 of normal *bcr* cDNA (8).

A region of normal *abl* mRNA from K562 cells (8) was amplified by reverse transcriptase PCR (9). The sequence of the *abl* cDNA primer is 5′ TAGGACTGCTCTCACTTCTCACG 3′. *Abl* specific cDNA was amplified by PCR. The sequences of the 5′ and the 3′ primers are 5′ ATCTGCCTGAAGCTGGTGGGCTGC 3′ and 5′ ATGCTTAGAGTGTTATCTCCACT 3′, respectively. The resulting PCR product maps from position 157 to position 340 of normal *abl* cDNA (5).

The normal *bcr* and *abl* PCR products were gel purified, phosphorylated and then blunt ended in the presence of dNTPs and the Klenow fragment of DNA polymerase. The DNA was then cloned into the *Hinc* II site of Bluescript II KS+.

Characterization of clones

Plasmid DNA was harvested from bacterial cultures according to an alkaline lysis protocol (10). Plasmid DNAs were characterized by both restriction enzyme and sequence analyses. Sequence analysis was carried out using Sequenase (United States Biochemical) and both the M13 $^{-}$20 and reverse primers according to conditions recommended by manufacturer.

Preparation of templates for T7 and T3 transcription

Plasmid DNAs were digested to completion with either *Hind* III, *Pst* I *Bam* HI, or *Xho* I (New England Biolabs) according to the manufacturer's directions. DNA was then digested with Proteinase K solution (Sigma) and resuspended in RNAase free H_2O at a concentration of 500 ng/μl. The template for the K28 substrate was a generous gift from Dr Scott Shore (Temple University, Philadelphia, PA).

In vitro transcription

The substrate and ribozyme RNAs were transcribed from the Bluescript II KS+ template using either T3 RNA polymerase (Promega) or T7 RNA polymerase (Promega) according to instructions provided by the manufacturer. Following transcription, the DNA templates were removed from the reaction by the addition of RNAase free DNAase (Worthington Biochemical) at 2 units per μg of DNA template and incubating at 37°C for 30 minutes. RNA was then digested with Proteinase K and resuspended in RNAase free H_2O.

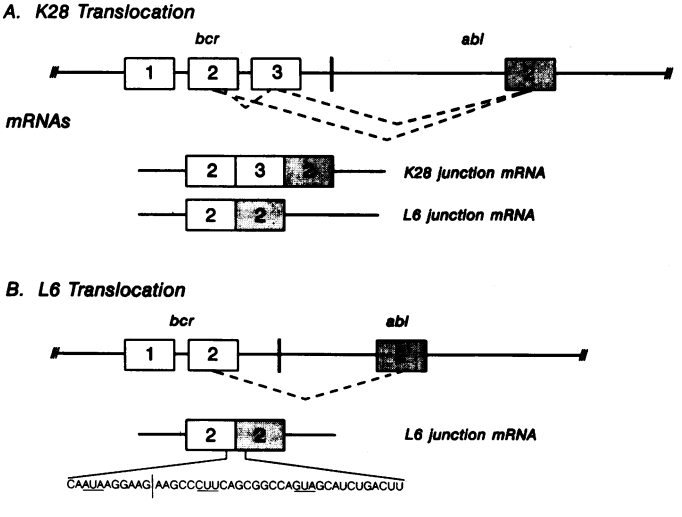

Figure 1. *bcr-abl* translocations and fusion mRNAs. The two types of chromosomal translocations that are associated with CML, and the associated fusion mRNAs, are depicted. **A**, K28 type translocation and fusion mRNAs; **B**, L6 type translocation and fusion mRNA. Unshaded boxes represent *bcr* exons and shaded boxes represent *abl* exon 2. Dotted lines connecting *bcr* and *abl* exons indicate alternative splicing pathways. The sequence of the L6 *bcr-abl* junction is expanded in Panel B. Potential ribozyme cleavage sites are underlined. The vertical lines indicate the position of the *bcr-abl* junction.

Substrate RNAs used as tracers in ribozyme cleavage experiments were radiolabelled during T7 or T3 transcription with [α^{32}P] CTP (Amersham) according to the manufacturers recommended procedure.

Ribozyme assays

Ten pmole of both ribozyme and substrate RNAs were incubated in 10μl of ribozyme reaction buffer (50 mM Tris−Cl, pH 7.5, 10 mM $MgCl_2$) containing 50,000 cpm of radiolabelled substrate RNA (specific activity [5×10^8cpm/μg]) as tracer. Reactions were incubated at 37°C for up to 10 hours and terminated by freezing on dry ice. Samples were subjected to denaturing polyacrylamide gel electrophoresis on 5% polyacrylamide gels (14). Gels were dried and subsequently analyzed with a PhosphorImager (Molecular Dynamics) according to the manufacturer's directions.

Gel shift analysis

Fifty pmole of ribozyme and 10 pmole of substrate were incubated in 10 μl of ribozyme reaction buffer containing 50,000 cpm of radiolabelled substrate RNA (specific activity [5×10^8cpm/μg]) at 37°C for 2.5 hours. Products were analyzed by native gel electrophoresis on a 6% polyacrylamide gel in 1× TBM buffer (90 mM Tris−borate, 10 mM $MgCl_2$). Gels were dried and subsequently analyzed with a PhosphorImager (Molecular Dynamics).

Kinetic analysis

Ribozyme reactions were carried out as described above but in the presence of substrate excess. The ribozyme concentration was held constant at 0.5 μM. The various substrate to ribozyme ratios used are described in the text and in Figure legend 6. Reactions were terminated at various times and the products subjected to denaturing gel electrophoresis. Gels were dried and subsequently analyzed with a PhosphorImager.

RNA folding

Secondary structures were predicted for ribozymes and substrate RNAs using the programs of Zucker and Steigler, on PC Gene (Intelligenetics) and MacDNASIS Pro (Hitachi).

Cells

K562 cells, which were used as a source of la *abl* mRNA, were obtained from the American Type Culture Collection (ATCC # CCL 243) and were cultured in complete minimal essential medium (JRH Biosciences) supplemented with 10% Fetal Bovine Serum (Gibco-BRL).

RESULTS

In vitro characterization of ribozyme cleavage

The L6(1) class of hammerhead ribozymes depicted in Figure 2A are the anchored ribozymes. The anchors which are located at the 3′ end of the ribozyme are complementary to the region of *bcr* exon 2 indicated in Figure 2A and are 31, 21, or 11 nts in length. Anchor sequences were inserted in order to favor hybridization to RNAs containing *bcr* sequences, thus discouraging the ribozyme from cleaving normal *abl* mRNAs. They are connected to the 5′ part of the ribozyme by means of a 13 nt spacer sequence. This spacer bears no complementarity to either *abl* or *bcr* sequences. The hammerhead catalytic core, located near the 5′ end of the ribozyme lies within a 15 nt sequence that is complementary to *abl* exon 2. A control ribozyme which lacks an anchor sequence but is otherwise identical to the anchored ribozymes, was also constructed.

These ribozymes have been designed to cleave the L6 *bcr-abl* mRNA at the GUA triplet located 19 nts 3′ of the *bcr-abl* junction. Cleavage at this site in the synthetic substrate generates two fragments which are 143 nt and 85 nts in length. Each of the ribozymes was able to cleave the L6 substrate into the expected cleavage products, and the amount of substrate cleaved

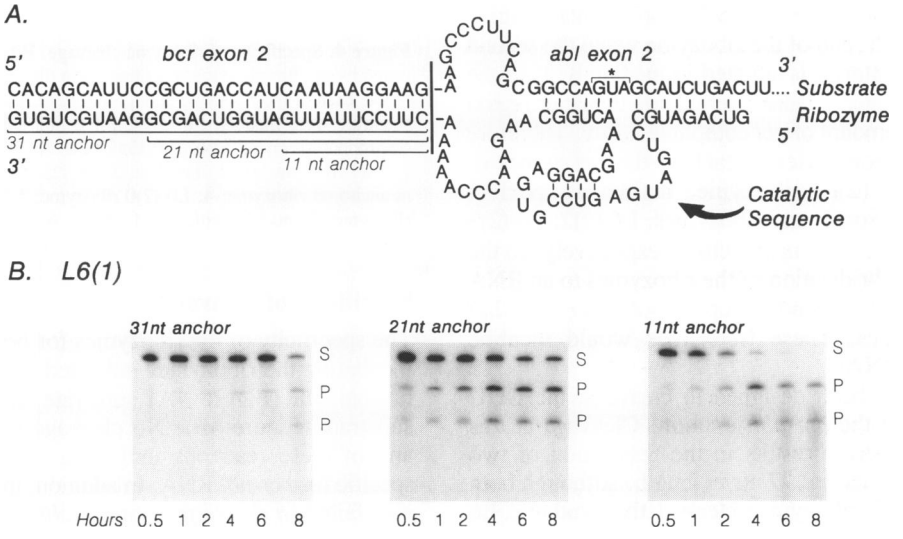

Figure 2. Time course of L6 substrate cleavage by the L6(1) anchored ribozymes. **A**, The L6(1) anchored ribozymes are shown with the L6 *bcr-abl* substrate. The length and sequence of the ribozyme anchors are indicated and the cleavage site in the substrate is indicated with a bracket and asterisk. The *bcr-abl* junction is indicated by the vertical solid line and base pairing between ribozyme and substrate is indicated by the small vertical lines. **B**, Substrate cleavage mediated by each anchored ribozyme. 10 pmole each of ribozyme and a mixture of radiolabelled and non-radiolabelled substrate were incubated at 37°C for the times indicated and subjected to denaturing electrophoresis on a 5% polyacrylamide gel. The substrate (S) and product (P) bands are indicated.

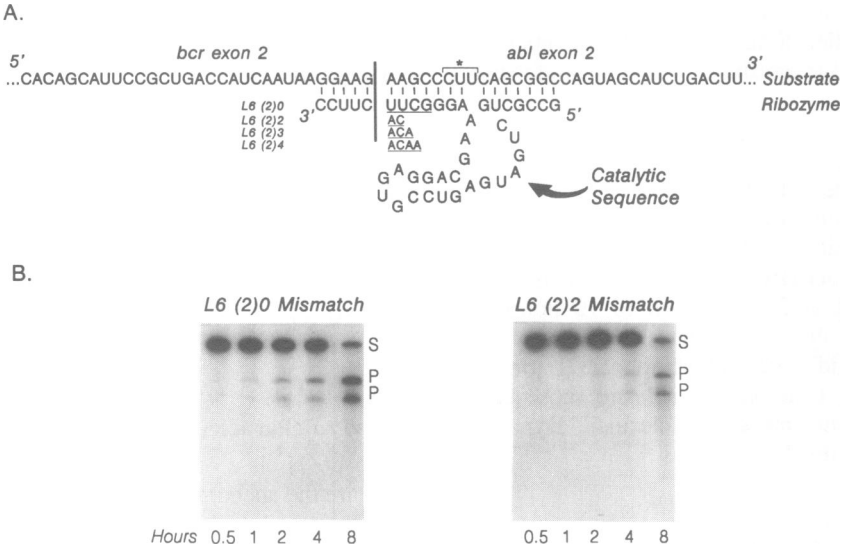

Figure 3. Time course of L6 substrate cleavage by the L6 (2) ribozymes. **A**, The L6 (2) ribozymes are shown with the L6 *bcr-abl* substrate. Nucleotide substitutions made in the ribozymes are indicated directly beneath the wildtype ribozyme sequence and are underlined. The ribozyme cleavage site is indicated with a bracket and asterisk, and the *bcr-abl* junction is indicated with a vertical solid line. Basepairing between ribozyme and substrate is indicated by small vertical lines. **B**, Substrate cleavage by the L6 (2)0 and the L6 (2)2 ribozymes is shown. 10 pmole each of ribozyme and a mixture of radiolabelled and non-radiolabelled substrate were incubated at 37°C for the times indicated followed by denaturing electrophoresis through a 5% polyacrylamide gel. The substrate (S) and product (P) bands are indicated.

by each ribozyme, was in general, inversely related to the length of the anchor sequence (Figure 2B). The 21 nt anchor ribozyme, however, demonstrated more activity than the 11 nt anchor ribozyme at the earlier time points. The anchor minus ribozyme also correctly cleaved the L6 substrate, however, cleavage was inefficient and only a small amount of product formation was observed (data not shown). No cleavage products were detected in the absence of ribozyme (data not shown).

The L6 (2) class of hammerhead ribozymes depicted in Figure 3A is comprised of a sequence complementary to *bcr* exon 2, the hammerhead catalytic core and two regions that are complementary to *abl* exon 2. The first *abl* complementary region is located at the extreme 5′ end of the ribozyme while the second region of *abl* complementarity is situated immediately 3′ to the catalytic sequence. Mismatches were inserted into the latter region in order to decrease the amount of *abl* complimentarity. Therefore the sequence of this region varies in each of the ribozymes of the series. The L6 (2)0 ribozyme maintains perfect complementarity to *abl* exon 2, and ribozymes, L6 (2)2, L6 (2)3 and L6 (2)4, contain 2, 3, or 4 mismatches, respectively, to the *abl* exon 2 sequence. Hybridization of the ribozymes to an RNA molecule might then be dependent upon both *bcr* and *abl* complementary sequences. These ribozymes would then be specific for *bcr-abl* mRNAs.

These ribozymes have been designed to cleave at the CUU triplet located 7 nt 3′ of the *bcr-abl* junction. Cleavage at this site in the synthetic substrate results in the generation of two fragments which are 131 nts and 97 nts in length. Although both the L6 (2)0 and L6 (2)2 ribozymes cleaved the synthetic L6 substrate into the expected cleavage products, the L6 (2)0 ribozyme was more active (Figure 3B). In addition, both ribozymes were also able to correctly cleave a synthetic K28 substrate as efficiently as they cleaved the L6 substrate (data not shown). The L6 (2)3 and L6 (2)4 ribozymes had no detectable activity (data not shown).

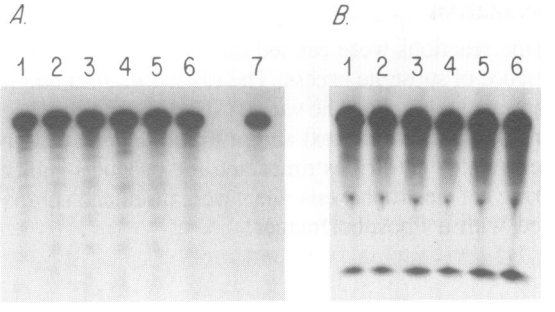

Figure 4. Specificity of ribozyme cleavage. Ribozyme cleavage specificity was tested by *in vitro* cleavage reactions using the normal *abl* and *bcr* substrates. 10 pmole each of the ribozyme and a mixture of radiolabelled and non-radiolabelled substrate were incubated at 37°C for 6 hours and subjected to denaturing gel electrophoresis on a 5% polyacrylamide gel. **A**, cleavage of the normal *abl* substrate 1, L6(1)31 nt anchored ribozyme, 2, L6(1)21 nt anchored ribozyme; 3, L6(1)11 nt anchored ribozyme; 4, L6 (2)0 ribozyme; 5, L6 (2)2 ribozyme; 6, L6 (2) 3 ribozyme; 7, no ribozyme. **B**, 1−5 see **A**, 6, no ribozyme.

Specificity of cleavage

The specificity of the ribozymes for *bcr-abl* RNA was tested by incubating the ribozymes indicated in Figure 4 with a synthetic normal *abl* (Figure 4A) substrate or a synthetic normal *bcr* substrate (Figure 4B). No cleavage products were detected in any of these reactions indicating that these ribozymes are all specific for *bcr-abl* RNA. In addition, the anchor-minus ribozyme also failed to cleave the normal *abl* substrate (data not shown).

Cleavage of normal *bcr* was not anticipated as this molecule lacks the target cleavage site, however, this target site is present in the normal *abl* substrate. Failure of the ribozymes to cleave this molecule may have been due to the inability of the ribozymes to bind to the normal *abl* substrate or to the inability of the ribozymes to cleave the molecule once bound to it. In order to

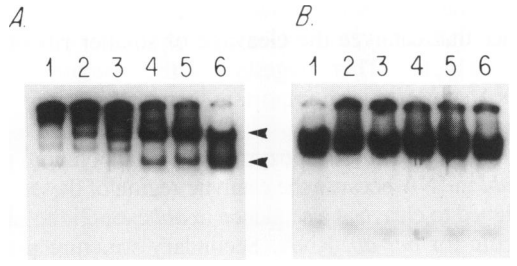

Figure 5. Analysis of ribozyme and substrate binding. The binding of each ribozyme to the L6 *bcr-abl* substrate and normal *abl* substrates was tested by a gel-shift assay. Fifty pmole of ribozyme and 10 pmole of a mixture of radiolabelled and non-radiolabelled substrate were incubated at 37°C for 2.5 hours and subjected to non-denaturing gel electrophoresis in the presence of 10 mM $MgCl_2$. Arrows indicate the positions of the two conformational species of the L6 *bcr-abl* substrate. **A**, ribozyme binding to L6 *bcr-abl* substrate. **B**, ribozyme binding to normal *abl* substrate. 1, L6(1) 31 nt anchored ribozyme; 2, L6(1) 21 nt anchored ribozyme; 3, L6(1) 11 nt anchored ribozyme; 4, L6 (2) 0 ribozyme; 5, L6 (2) 2 ribozyme; 6, no ribozyme.

discriminate between these two possibilities, a substrate gel shift assay was performed.

Ribozyme–substrate binding studies

Gel shift experiments were performed with either a radiolabelled L6 *bcr-abl* substrate (Figure 5A) or a radiolabelled normal *abl* substrate (Figure 5B). Two predominant conformational species of the L6 *bcr-abl* RNA exist under the assay conditions (Figure 5A, lane 6). Both of these species were shifted by the three anchored ribozymes (Figure 5A, lanes 1, 2 or 3). In contrast the L6 (2)0 and the L6 (2)2 ribozymes were only able to shift the faster migrating species of *bcr-abl* RNA (Figure 5A, lanes 4 and 5). None of the ribozymes tested was able to shift the radiolabelled *abl* substrate which migrates as one conformational species on a native gel (Figure 5B, lanes 1–6). This result indicates that the specificity of these ribozymes for the *bcr-abl* substrate was due to the inability of these ribozymes to bind to the normal *abl* substrate.

Kinetic analysis of ribozyme reaction rates

A kinetic analysis was performed to identify ribozymes with higher rates of reaction. The 21 nt and 11 nt-anchored ribozymes were initially chosen for further analysis because they exhibited not only specificity but also the highest rates of cleavage at the early time points (Figure 2B and 3B). This analysis would also enable us to determine the effect of anchor length on ribozyme activity.

All experiments were carried out under conditions of substrate excess. Cleavage rates were determined for the 11 and 21 nt anchored ribozyme in reactions containing the three ratios of substrate to ribozyme indicated in Figure 6A and B. Analysis of the results suggested that these reactions did not follow Michaelis–Menton kinetics (11). The data were therefore fitted to pseudo-first-order kinetics by plotting the ratio of the concentrations of product and ribozyme against time (Figure 6A, B, C). Reaction rates were obtained from the linear regression of the reaction time course using the 'Enzyfitter' program (Elsevier Biosoft). Both ribozymes exhibited a burst of product formation at early time points followed by a much slower steady state rate. The slope of the initial burst indicates the catalytic rate to be 0.03/min for each ribozyme. The slope at later timepoints indicates the dissociation rates of the products from

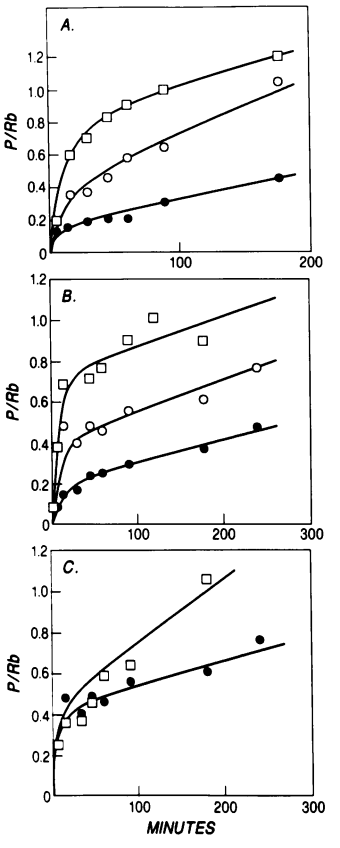

Figure 6. Analysis of ribozyme reactions fitted to pseudo-first order kinetics. The concentration of product (P) normalized to ribozyme (Rb) concentration is plotted versus time. **A**, L6(1) 11 nt anchored ribozyme; **B**, L6(1) 21 nt anchored ribozyme. The ratios of substrate to ribozyme in the reactions were as follows: ● 2:1; ○ 5:1; □ 10:1. **C**, The kinetics of the L6(1) 11 and L6(1) 21 nt anchored ribozymes □, ● respectively, at a substrate to ribozyme ratio of 5:1 are compared.

the ribozyme. Similar slopes were observed at the various ribozyme to substrate ratios for a given ribozyme. However, at all substrate to ribozyme ratios tested, the 21 nt anchored ribozyme exhibited a 3- to 4-fold slower turnover than the 11 nt ribozyme as indicated by the differences between the two slopes (Figure 6A, B, and C).

DISCUSSION

Ribozymes cleave at motifs found in most mRNA molecules and have been made specific for an mRNA by targeting the ribozyme to sequences immediately flanking the selected cleavage site (12). However, it might sometimes be desirable to cleave an RNA molecule at a sequence located a distance from the sequence used to target the ribozyme. Here we demonstrate an approach that allows a ribozyme to be targeted to sequences that are non-contiguous with the cleavage site.

We have used the chimeric L6 *bcr-abl* RNA, the expression of which is believed to be important in the establishment of CML, as a model for our approach. Although this fusion mRNA contains multiple ribozyme cleavage sites, the sites are flanked by sequences found in normal *abl* or *bcr* mRNAs. A ribozyme targeted to any of these cleavage sites would therefore have the potential to cleave the normal *abl* and *bcr* mRNAs as well as the aberrant *bcr-abl* mRNA. An anchor sequence comprised of

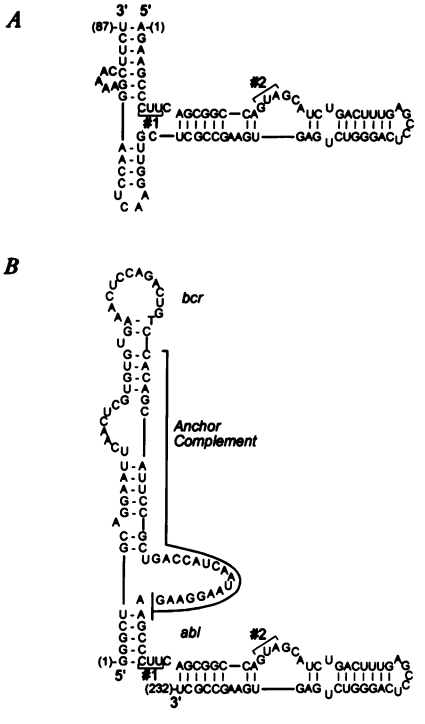

Figure 7. Secondary structure predictions. Secondary structure predictions for substrate RNAs were generated using the Zucker and Steigler algorithm for RNA folding. The complete nucleotide sequence of the synthetic substrate molecules was analyzed, however, only a portion of the folded structure is presented. The anchor complement and substrate cleavage sites are indicated. #1 and #2 indicate the two ribozyme cleavage sites CUU and GUA, respectively. The *bcr-abl* junction in the L6 *bcr-abl* substrate is indicated by the vertical line between AAG|AAG and the numbers in parenthesis indicate the first and last nucleotide in the presented structure. **A**, Normal *abl* substrate, nt 1−87 are derived from *abl* exons 1a and 2. **B**, L6 *bcr-abl* substrate, nt 1−14 are derived from the Bluescript polylinker sequence, nt 15−72 are derived from *bcr* exon 2, and nt 73−232 are derived from *abl* exon 2.

bcr complementarity was therefore inserted into the ribozymes designed to cleave L6 *bcr-abl* mRNA at a more distant GUA triplet located in *abl* exon 2. The anchor was inserted in an attempt to localize these ribozymes to RNAs containing *bcr* sequences. The only molecules containing *bcr* sequences that should be cleaved are those which also contain the *abl* exon 2 specific cleavage site and flanking sequence.

The presence of an anchor sequence could potentially have a detrimental effect on ribozyme activity by either causing the ribozyme to fold incorrectly or by compromising recycling of the ribozyme. Therefore ribozymes containing anchors of various lengths were tested for cleavage activity. Although none of the anchor sequences prevented the correct cleavage of the L6 substrate, kinetic analysis indicated that product release, the rate limiting step in the cleavage reactions, was slower in reactions catalyzed by ribozymes with longer anchors. The initial burst rate was similar for both the 11 nt anchored and the 21 nt anchored ribozyme when reactions were carried out under conditions of substrate excess. The 21 nt anchored ribozyme has a slower product dissociation rate than does the 11 nt anchored ribozyme, and the net result is that the 11 nt anchored ribozyme is more efficient over an extended reaction time. The measured rates are similar to the reported rates of other ribozymes that catalyze the cleavage of relatively large RNA substrates (13). However, these rates are slower than the rates measured for ribozymes that catalyze the cleavage of smaller ribonucleotide substrates (14,15). This suggests that the structure and length of an RNA substrate is an important factor which may influence ribozyme rates.

Although the anchored ribozymes have the potential to cleave normal *abl* mRNA because the catalytic region of these molecules was designed to cleave at a sequence in *abl* exon 2, the ribozymes are specific for *bcr-abl* RNA. Secondary structure predictions for normal *abl* RNA suggest that the sequences flanking the cleavage site may not be accessible for ribozyme binding (Figure 7A). This was confirmed experimentally utilizing an *in vitro* binding assay. We predicted that the ribozymes would cleave the normal *abl* substrate if the secondary structure of the substrate was first melted. Experiments were therefore carried out in which the substrate was first denatured and then renatured in the presence of ribozyme. Under these conditions, between 15 and 20% of the normal *abl* substrate was cleaved by the 11 nt anchored ribozyme (data not shown). This result together with the gel shift data support the interpretation that the normal *abl* substrate is folded in a way that occludes ribozyme nucleation. It is therefore likely that the anchored ribozymes failed to cleave normal *abl* RNA because it is inaccessible for ribozyme binding.

Secondary structure predictions for the L6 *bcr-abl* substrate suggest that the sequences flanking the ribozyme cleavage site are also inaccessible for ribozyme binding but that most of the region complementary to the ribozyme anchor is available for anchor hybridization (Figure 7B). Although these predictions were generated for a substrate RNA that contains a vector derived polylinker sequence, predictions made for the native substrate RNA indicated that most of the anchor complement is available in this molecule as well. According to our model, the function of the ribozyme anchor is to tether the ribozyme to an accessible substrate sequence thereby sequestering the molecule in the vicinity of the substrate cleavage site. This would allow the ribozyme to cleave the substrate whenever the cleavage site and flanking sequences become available due to temporary transitions in secondary structure.

Although we have used a chimeric RNA to demonstrate the utility of a ribozyme anchor in overcoming an obstruction caused by the secondary structure around a cleavage site, an anchor could potentially be used to target ribozymes to occluded sites in any RNA molecule. An anchor may also be used to increase the specificity of a ribozyme for a chimeric RNA.

The smallest anchor we have tested was 11 nucleotides long, but the optimal length of an anchor may be less than this and is probably dependant upon the anchor sequence and the secondary structure. The presence of some form of anchor is clearly important as inefficient cleavage was observed with a conventional ribozyme, the anchor-minus ribozyme. The anchors we have tested are all attached to the ribozyme via a 13 nucleotide spacer. Anchors might also be connected via a chemical spacer or simply linked directly to the ribozyme. The presence of a spacer may be sterically important in cases in which a ribozyme is tethered at a position distant from the cleavage site.

A second approach was taken in the design of the L6 (2) ribozymes. These ribozymes were designed to cleave *bcr-abl* mRNA at the CUU triplet located 7 nucleotides 3′ of the *bcr-abl* junction. This site is also present in normal *abl* mRNA, however, and the ribozymes thus have the potential to cleave this RNA as well. Therefore a series of mismatches in *abl* complementarity was introduced into the ribozymes in an attempt

to discourage cleavage of normal *abl*. These ribozymes also contain 5 nucleotides of complementarity to a region in *bcr* exon 2 present in the *bcr-abl* mRNA. It was thought that successful binding of one of these ribozymes would be dependant upon binding of both *bcr* and *abl* complementary sequences. In this case the ribozyme would be specific for *bcr-abl* mRNA.

The only ribozymes of this series that demonstrated any activity were the L6 (2)0 and the L6 (2)2 ribozymes. The L6 (2)0 ribozyme was more active than the L6 (2)2 ribozyme. These ribozymes were specific for the *bcr-abl* RNA but were not as active as the anchored ribozymes in cleavage reactions analyzed at early time points. The lower activity of the L6 (2) ribozymes was, in part, due to reduced substrate binding as is demonstrated by the gel shift assay. These ribozymes appeared to bind significantly to only one of the conformational species of the L6 *bcr-abl* substrate. However, most of the substrate was cleaved by the L6 (2)0 ribozyme after 8 hours suggesting that the secondary structure of the substrate may not be static and may shift into another conformation that allows ribozyme binding.

In order to understand the possible interactions between the L6 (2) ribozymes and the L6 *bcr-abl* substrate, the secondary structure predictions generated for the substrate RNA were analyzed (Figure 7B). These predictions indicate that the cleavage site and flanking *abl* sequence recognized by the L6 (2) ribozymes may not be accessible to these ribozymes (Figure B). However, a region of *bcr* complementary to the 3′ end of the ribozymes as well as one nucleotide of *abl* does appear to be accessible in the predicted RNA conformation. This region may not be available in the second conformational species of the L6 substrate RNA that is not bound by the ribozymes. These results suggest that the *bcr* complement plus the one *abl* nucleotide complement may be functioning as a 6 nt anchor sequence. Accordingly, a ribozyme lacking this 6 nt sequence was found to be less efficient than the L6 (2)0 ribozyme at cleaving the *bcr-abl* RNA. (data not shown).

Both the L6 (2)0 and L6 (2)2 ribozymes were also able to cleave a synthetic K28 substrate as efficiently as they cleaved the L6 substrate (data not shown). These molecules are the first reported to specifically cleave both the L6 and the K28 fusion mRNAs and thus could potentially be used to treat cases of CML associated with either a K28 or L6 type translocation.

In conclusion, we have demonstrated novel approaches for ribozyme targeting. This approach makes it possible to target ribozymes and possibly antisense oligonucleotides to cleavage sites that would otherwise be inaccessible due to the secondary structure of the substrate RNAs. These same approaches may also increase the specificity of a ribozyme or an antisense oligonucleotide for a chimeric RNA. Using this approach, several ribozymes have been designed that may be useful in the treatment of CML. Experiments are in progress to test the activity of these ribozymes in established CML tissue culture lines.

ACKNOWLEDGEMENTS

We would like to thank Dr Fred Oakes, Gregory Stratton, and Stephen Marino for oligonucleotide synthesis and purification, David M.Sanborn and Daniel V.Zurawski for help in sequence analysis, and Dr Susan Weiss and Dr C.Satishchandran for aid in data analysis. We also gratefully acknowledge Kathleen M.Herold for critical review of the manuscript and Monica Sinquett and Heather Kirkpatrick for help in the preparation of the manuscript.

REFERENCES

1. Nowell,P.C., and Hungerford,D.A. (1960) *Science*, 132, 1497–1499.
2. Rowley,J.D. (1973) *Nature*, 243, 290–293
3. Groffen,J., Stephenson,J.R., Heisterkamp,N., de Klein,A., Bartram,C.R., and Growveld,G. (1984) *Cell*, 36, 93–9.
4. Heisterkamp,N., Stephenson,J.R., Groffen,J., Hansen,P.F., de Klein,A., Bartram,C.R., and Grosveld,G. (1983) *Nature*, 306, 239–242.
5. Shtivelman,E., Lifshitz,B., Gale,R.P., Roe,B.A., and Canaani,J. (1986) *Cell*, 47, 277–284.
6. Beaucage,S., and Caruthers,M. (1981) *Tetrahedron Lett.*, 22, 1859–1862.
7. Heisterkamp,N., Stam,K., and Groffen,J. (1985) *Nature*, 315, 758–761.
8. Lozzio,C.B., and Lozzio,B.B. (1975) *Blood*, 45, 321–334.
9. Innis,M.A., Gelfand,D.H., Sninsky,J.J., and White,T.J. (1990) *PCR Protocols, A Guide to Methods and Applications*, Academic Press, Inc., San Diego, CA.
10. Sambrook,S., Fritsch,E.F., and Maniatis,T. (1989) *Molecular Cloning, A Laboratory Manual*, 2nd Ed., Cold Spring Harbor Press, Cold Spring Harbor, NY.
11. Boyer,P.D. (1970) *The Enzymes*, Student Ed., Academic Press, Inc., New York, NY.
12. Haseloff,J., and Gerlach,W.L. (1988) *Nature*, 334, 585–591.
13. Taylor,N.R., and Rossi,J.J. (1991) *Antisense Res. Dev.*, 1, 173–186.
14. Fedor,M.J., and Uhlenbeck,O.C. (1990) *Proc. Natl. Acad. Sci. USA*, 87, 1668–1671.
15. Fedor,M.J., and Uhlenbeck,O.C. (1992) *Biochemistry*, 31, 12042–12054.